



Reconstruction of the 1989 Laguna Del Cerro Largo GLOF: an Interdisciplinary Understanding of GLOF Impacts

Jonathan Burton¹, Frederick Chambers¹, Lisa Kelley¹, Benjamin Soto Narbona²

¹Geography and Environmental Science, University of Colorado, Denver, 80204, USA

⁵ ² La Facultad de Historia Geografía y Ciencia Política, Pontificia Universidad Católica de Chile, Santiago, Chile

Correspondence to: Jonathan Burton (jonathan.burton@ucdenver.edu)

Abstract. The March 16, 1989, glacial lake outburst flood (GLOF) from Laguna del Cerro Largo in Valle Soler, Aysén, Chile, is one of the largest recent moraine-dammed GLOFs in the region. This interdisciplinary approach reconstructs the GLOF downstream impacts using HEC-RAS 2D and GeoClaw from witness accounts. Model results are then validated through field analysis of sediment deposition, dendrogeomorphic surveys, radiocarbon dating. Sediment cores reveal distinct clastic layers attributable to the 1989 event and evidence of an earlier outburst flood from the adjacent Laguna Turbio, dated circa 125 ybp. The model results also indicate a substantially higher peak discharge than official reports, impacting subsequent disaster policy decades later. While dendrogeomorphic sampling was hindered by fungal decay in Nothofagus species, the findings highlight both the potential and limitations of interdisciplinary reconstructions of GLOF events in remote, data-scarce environments.

15 1 Introduction

Glacial lake outburst floods (GLOFs) are a growing concern in glacierized regions and their downstream watersheds, with an estimated 15 million people at risk globally (Taylor et al., 2023). These events pose substantial hazards, redistributing millions of cubic meters of sediment, destroying infrastructure, and threatening lives (Clague et al., 2012; Taylor et al., 2023). Yet significant uncertainties persist concerning their climate sensitivity (Harrison et al., 2018), anthropogenic drivers (Huggel et al., 2020), and magnitude (Rick et al., 2023; Veh et al., 2025), among other characteristics. Research on adaptation and response also varies widely (Carey et al., 2021; Colavitto et al., 2023), with findings that are at times contradictory (Chen et al., 2025; Rounce et al., 2017). These challenges are compounded by growing uncertainty over the future scale and intensity of environmental shifts driven by climate change (Hock & Truffer, 2024).

The current narratives of GLOF hazard stand in stark contrast to the historical treatment of GLOFs in Chilean Patagonia. Until recently, state and regional governments gave little attention to GLOFs as hazards requiring mitigation; instead, such events were largely accepted as an inherent feature of life in a peri-glacial environment. Although the region has experienced hundreds of GLOFs over the past century (Lützow et al., 2023), Patagonia remains significantly understudied, in part due to its rural character and low population density. However, this historical inattention contrasts sharply with projections of increasing future risk. GLOF frequency and impact are expected to rise in coming decades (Zhang et al., 2024), with continued glacial



30 lake expansion and a projected 26 to 41 percent reduction in glacier mass by 2100 under warming scenarios of 1.5 to 4 degrees Celsius (Rounce et al., 2023; Schuster et al., 2025). This persistent lack of research attention, coupled with unresolved uncertainties surrounding GLOF dynamics and hazard extent, continues to impede effective adaptation and risk governance in the region.

35 On March 16, 1989, a large GLOF inundated Valle Soler, an isolated glacial drainage on the eastern margin of the Northern Patagonia Icefield (Figure 1). The flood destroyed three homes, damaged dozens of other homes and property, and killed “a great quantity” of livestock (Hauser, 1993), originating from the failure of a moraine dam retaining Laguna del Cerro Largo (LCL). The flood was one of the largest recent moraine-dammed GLOFs by volume and estimated discharge (Clague & Evans, 2000), even reversing the flow of the Rio Baker—Chile’s largest by volume—for several hours. Yet the event received little scientific attention beyond an initial field study (Hauser, 1993) and brief mentions in the broader GLOF literature (Clague &

40 Evans, 2000; Iribarren Anacona et al., 2014).



Figure 1. Laguna del Cerro Largo and Valle Soler in the Aysén region of Chile. The initial impact zone of the 1989 GLOF is visible in the first 15 km with extensive sediment mobilization and deposition. Powered by Esri.

Here we undertake an interdisciplinary investigation of the 1989 Valle Soler GLOF, drawing on diverse methods to examine 45 both the historical and ongoing impacts of the event. We highlight how integrating physical and local knowledge can improve hazard interpretation and governance in data-sparse mountain regions. While GLOFs are often treated as geophysical phenomena, they also mobilize policy and development planning for disaster risk reduction, requiring approaches that account for both physical and socio-political dimensions of change. To better understand the 1989 GLOF, we present a 27 km² digital elevation model (DEM) derived from an unmanned aerial vehicle (UAV) drone, numerical modeling of GLOF hydrologic 50 dynamics, and field sediment and dendrogeomorphic samples from a field excursion undertaken in the austral summer of 2024. These diverse datasets comprise a history of GLOF impacts in order to advance considerations of the ongoing impacts on disaster and risk policy today.



55 1.1 Study Area

The Aysén region of Chile is home to some 10,300 glaciers, with approx. 8700 km² of glacial surface area (IPG, 2022). Glaciers have retreated dramatically over the past century, consequent to anthropogenic climate change (Dussaillant et al., 2019; Hugonnet et al., 2021). Since 1870, glaciers around the Northern Patagonia Icefield have lost 25% (East margin of NPI) and 60 11% (West margin of NPI) of their LIA ice extent (Carrivick et al., 2024). Glaciers along the eastern margin of the NPI have experienced stronger rates of decrease (Carrivick et al., 2024; Dussaillant et al., 2018) while glacial retreat along the western margin have been mitigated in part by increases in frozen precipitation, offsetting the net loss of glacier mass (Troch et al., 2024).

As glaciers retreat across Patagonia, the number and size of glacial lakes continue to grow, with a 27% increase of glacial lake area from 1986 to 2016 (Wilson et al., 2018). This expansion has heightened concern over GLOFs, which have occurred 65 hundreds of times in the region over the past century (Lützow et al., 2023). Many of the GLOFs that have occurred in Patagonia are located in relatively remote valleys with low or little downstream populations, but have killed livestock, and destroyed barns, houses, bridges, and roadways (Iribarren Anacona et al., 2015, 2023; Jacquet et al., 2017; Torrejón and Bertrand, 2021). However, GLOF hazard exposure is expected to increase due to ongoing development and shifting land use dynamics 70 (Dussaillant et al., 2010; Hock et al., 2019). In Aysén, a recent influx of external investment and infrastructure expansion is rapidly transforming long-standing social and territorial relationships. These changes are especially pronounced in struggles over land governance, where global economic forces have collided with local traditions and rural livelihoods (Blair et al., 2019). The convergence of accelerated socio-economic development and climate change has prompted profound shifts in state-society relations and reshaped the political landscape of land governance.

2 Methodology

75 A mixed-methods approach was used in this study, integrating data spanning several years of field work in Aysén. The research involved close collaboration with local community members and followed principles recommended for community-based research (Pearce et al., 2009). Traditionally, flood reconstructions rely on the evidence of analysis acquired through a single discipline, limiting the insights of flood source, pathway, and impact (Williams et al., 2022). This research triangulates diverse data, including UAV-derived DEMs, dendrogeomorphic sampling, sediment analysis, and oral histories to build a composite 80 case study of the 1989 GLOF, adopting what Nightingale calls ‘epistemological pluralism’ (2016). This research combines diverse types of data and perspectives to explore where findings align and where they diverge, lending insight into the ongoing impact of this event on disaster policy.

2.1 Witness Interviews

The 1989 GLOF occurred in a remote and sparsely populated valley in rural Aysén, with only a few individuals present to 85 witness the event firsthand. To document these accounts, I conducted interviews with the three surviving witnesses who were present in the valley at the time. These interviews aimed to capture witness descriptions of the flood’s magnitude, timing,



spatial extent, and other qualitative characteristics, in order to accurately model the event. Questions focused on the individual's experience of the event, where they were located, and flood characteristics at specific points in the valley (e.g., depth, duration, magnitude of flood extent), and the immediate aftermath. Additional questions addressed perceived impacts, 90 government response, and adaptive actions, offering insights into how the event was understood locally and how institutional responses unfolded in its wake.

2.2 Hydrologic Flood Modeling

This study compared two flood models, HEC-RAS 2D and GeoClaw (version 5.9.0, 2018) to simulate the March 1989 flood. The two modeling programs use comparable but distinct input conditions and parameters, which lead to differences in their 95 resulting outputs which are discussed in continuation.

Both hydrologic flood models used Copernicus 30m data for the input DEM to minimize bias in the model comparison. The Copernicus DEM is derived from the TanDEM-X mission and was acquired between 2010 and 2014 and released for public use in 2019. The DEM area is approximately 480.2 km², spanning the length of the impacted valley. For both models, witness 100 accounts provide details used to derive flood characteristics and, in select locations, for approximations for paleo-stage indicators. Field expeditions evaluated these paleo-stage indicators and validated model results via geomorphologic stage indicators. The DEM used in the modeling was generated after the flood event, which affects the accuracy of the topographic representation by reflecting post-flood terrain alterations that influence channelization and flow pathways. The flood simulations assume that (1) the topographic boundary for the flood is the water surface and valley walls (according to witness 105 accounts of flood behavior), and (2) ignore any topographic changes that may have occurred consequent of flood deposition/erosional forces.

This comparison aimed to achieve two primary objectives. First, to estimate key flood characteristics—such as extent, timing, and peak discharge—using established modeling approaches. Second, to evaluate the influence of model structure by comparing outputs generated from similar input conditions where possible. For instance, while HEC-RAS 2D requires a hydrograph to initiate the simulation, GeoCLAW relies solely on a specified bulk volume of drained water. The implications 110 of these differing input requirements, along with initial assumptions, are discussed in detail in the following subsections.

2.2.1 HEC-RAS 2D

Input condition parameters are fundamental to accurately determine key flood characteristics such as peak discharge. While parametric equations have been used to estimate input parameters that are often difficult to measure (Allen et al., 2017; Somos-Valenzuela et al., 2016; Westoby et al., 2014), several studies have found outflow hydraulics to be highly sensitive to initial 115 input conditions (Rinzin et al., 2025; Sattar et al., 2021; Wahl, 2004). Contrasting with initial reports for this event (Hauser 1993), hydrologic modeling suggests a much larger peak discharge occurred, supported by witness accounts (Burton et al., 2020). This study builds on previous work (Burton et al., 2020) to characterize the 1989 GLOF event. Witness interviews from three accounts (S1) provide the foundational description of flood development, propagation downstream, and flood time (used here as the Δ time of noticeably raised river water).



120 HEC-RAS 2D has been successfully employed for GLOF reconstruction (Iribarren Anacona et al., 2015; Klimeš et al., 2014; Kougkoulos et al., 2018; Sattar et al., 2021; Wang et al., 2024), and is capable of simulating multidirectional and multi-channel flows, which are characteristic of GLOFs. One significant advantage is the ability to simulate moraine dam failure through the dam-break module (W. Wang et al., 2018). HEC-RAS 2D solves the Saint-Venant equations, making it suitable for modeling flood routing across complex and steep terrain. However, these equations assume shallow, Newtonian flow which limits the
125 model's ability to represent GLOFs that carry large amounts of sediment or debris.

We modeled the failure of the Laguna del Cerro Largo, designating the storage area (lake) and moraine dam (boundary) as the boundary conditions. The discharge hydrograph was estimated using the total flood volume calculated from Burton et al. (2020), derived from the bulk volume ($\sim 140 \times 10^6 \text{ m}^3$) over the 8 hours of elevated flood waters as described from witness accounts. We compared Q_p to parametric equations established within the literature, with $20,000 \text{ m}^3/\text{s}$ most closely matching
130 the observed impacts (see Burton et al., 2020). Dam failure time (T_p, h) was estimated as follows (Froehlich, 1995):

$$T_p = 0.00254V^{0.53}h_b^{-0.9} \quad (1)$$

where V is the outburst volume (m^3) and h_b is the breach height (m). This flow hydrograph was then used as an upstream boundary condition for the downstream 2-dimentional GLOF routing. We allowed the simulation to run for 24 hours to ensure the simulation ran in its entirety.

135 2.2.2 GeoCLAW

The second model used to simulate the 1989 event is GeoClaw, a hydrodynamic model designed to efficiently solve the shallow water equations over complex topography. GeoClaw, like HEC-RAS 2D, solves the two-dimensional Saint-Venant equations (Berger et al., 2011), but distinguishes itself through its use of Adaptive Mesh Refinement (AMR). This technique dynamically concentrates computational grid cells in areas of rapid change—such as along the advancing flood wave—while maintaining
140 coarser resolution elsewhere. AMR allows for a computationally efficient yet high-resolution simulation of flood wave propagation.

The coarse level-1 rectangular grid with a resolution of $\sim 500 \text{ m} \times 150 \text{ m}$ covers the extent of the computational domain, a rectangle of size $14 \times 35 \text{ km}$, or approximately 480 km^2 . Four additional levels of refinement are user-defined input parameters, each at successive factors of 2, such that level-5 refinement is $\sim 10 \text{ m}$. Unlike HEC-RAS, GeoClaw assumes an instantaneous
145 dam failure, creating an artificial wall of water that, upon initiating the flood, calculates the flood wave propagation through the downstream terrain. The AMR capabilities enhance the accuracy and efficiency of modeling by dynamically adjusting the resolution of the computational grid based on specific local conditions during a simulation. The instantaneous release of water is, of course, not reflective of the real and complex processes chains entailed by moraine dam incision and reflects an overestimate of downstream impacts. However researchers have successfully used the model to simulate highly dynamic
150 GLOF conditions (Turzewski et al., 2019).



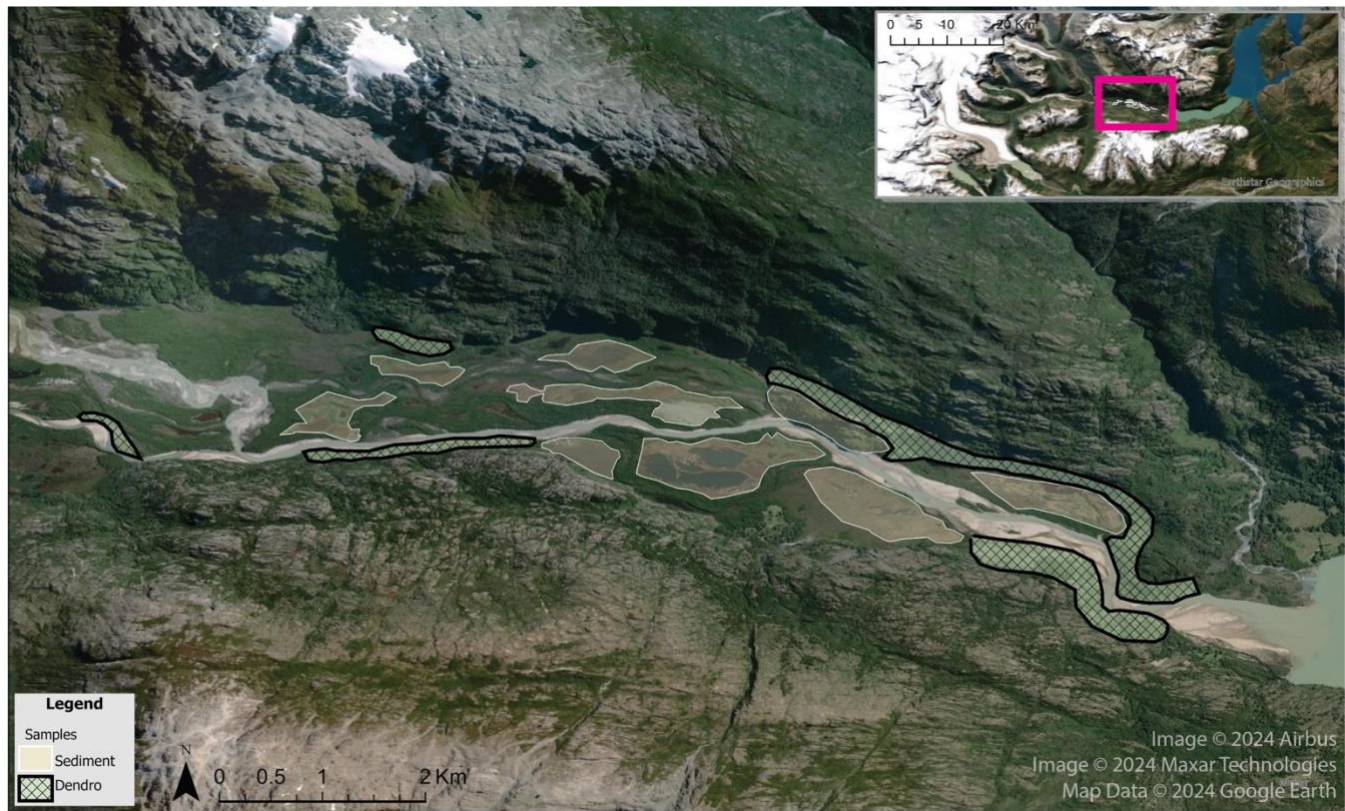
2.3 Unmanned Aerial Vehicle derived Digital Elevation Model

In order to analyze geomorphologic impacts from the 1989 GLOF of Valle Soler, we generated a digital elevation model (DEM) from photogrammetry using a DJI Mavic 2 Pro equipped with a high-resolution camera (4000 x 2250 pixels). A total of 18 separate UAV flights mapped the end moraine of the Laguna of Cerro Largo and the visible downstream deposition from 155 the 1989 GLOF, covering an area of 6.58 km². We prepared the UAV flights using PIX4Dmapper and flew at an altitude of 300m, with a few missions varying ± 100 m to account for strong winds or to avoid steep canyon walls. The UAV cameras were oriented at 75° (15° off nadir) to accurately image steep terrains such as canyon walls terminal moraine faces. Each UAV 160 mission is flown on a double pass grid, capturing images from two perpendicular angles, and maintained >80% overlap between images to ensure comprehensive coverage. To ensure accuracy and scale, ground control points (GCP) were distributed throughout the target area. UAV acquired images were processed with PIX4Dmapper software to produce a high-resolution 2D orthomosaic, a Digital Surface Model, and a Digital Terrain Model. The final DEM had a spatial resolution of approximately 12 cm/pixel.

2.4 Field Validation

Witness testimonies state that the propagating flood wave filled the valley from wall to wall and contained a slurry of sediment-165 laden and woody material. This is plainly evident in the initial stretches (< 10-12 km) of the valley (Figure 1), but these indicators, characteristic of GLOF flows, are more difficult to detect from remote sensing technology and noticeably diminish at ~ 15 km downstream. At ~ 12 km downstream, visible signs of sediment deposition largely disappear, seemingly inconsistent with the magnitude of the GLOF. Emmer (2023) discusses the methodological and ontological complexity of vanishing 170 evidences of GLOF events, a paradox which motivated the current analysis. For this reason, a sedimentological and dendrologic sampling field campaign was undertaken to compare with the results of the numerical modeling of the GLOF event.

Sampling sites were selected based on anticipated flood impacts, including low-energy environments conducive to sediment deposition and high-energy zones likely to produce dendrogeomorphic evidence of disturbance (Figure 2). Samples were collected during the same field campaign and are discussed separately in continuation.



175

Figure 2. Map of identified potential sampling sites for both sediment (tan) and dendrogeomorphic (hatched light green) of the lower Valle Soler.

2.4.1 Sediment Samples

Following Vandekerkhove (2020), likely zones of sediment deposition were identified through analysis of the downstream 180 glaciofluvial valley. A suitability analysis in the Valle Soler identified regions that were accessible and increased likelihood of successful sample extraction. The following characteristics were used to identify these regions:

Table 1. Sediment Sample Extraction Characteristics

Characteristic	Underlying Logic
Immediately adjacent to a major water drainage	Initial reports estimated $\sim 2\text{ k m}^3\text{s}^{-1}$ discharge, substantial, but not enough to fill the valley. Selecting sites close enough to the river to be impacted by a large magnitude event increased likelihood of positive identification and sample extraction.
Outside the interannual fluvial floodplain	Sufficient distance so as to minimize likelihood of disturbance from large magnitude (non-GLOF) flooding.
Relatively flat, low-lying environment	Prioritizing low-energy environments where deposition of finer sediments is increased. Also minimizes disturbances from tree roots to facilitate sample extraction.



Where possible, prioritize areas immediately preceding or following constrictions in the valley walls	Chokepoints in drainage channels cause water to accelerate through the constriction. This causes upstream pooling (creating backwater effects) or generate downstream eddies due to the decrease in velocity. In both situations, sediment tends to accumulate in these areas and were prioritized for sampling sites.
-------------------------------------------------------------------------------------------------------	------------------------------------------------------------------------------------------------------------------------------------------------------------------------------------------------------------------------------------------------------------------------------------------------------------------------

185 We extracted samples from *humedales*, a type of peat wetland present throughout the periglacial landscapes of Patagonia, with a Russian Peat Auger (RPA) and Soil Probe (Figure 3). The RPA is a hollow steel tube, attached to a steel handle, with one side covered by a metal sheath that, when inserted into water saturated sediment, is rotated to separate the sediment sample from the ground matrix so that the now enclosed sediment can be extracted. This sampling method preserves the small-scale depositional structures and stratigraphy of the soil, and has been used to analyze GLOF deposits (Vandekerkhove et al., 2020).
190 The soil probe is a simpler contraption that was used primarily as an initial probe into the soil to test if the RPA would be appropriate. In some locations, we were unable to insert the RPA into the ground but were able to extract smaller samples with the soil probe.



195 **Figure 3. Russian Peat Auger (RPA) used in the field. The auger is pushed into substrate (top-right), and rotated to close the gate, isolating the sediment core from the substrate.**

2.4.2 Dendrogeomorphic Samples

Dendrogeomorphology is the analysis of tree-rings and growth patterns to understand geomorphologic processes, and has been successfully used to date and analyze floods (Ballesteros-Cánovas et al., 2015; Casteller et al., 2015), debris flows



(Bollschweiler and Stoffel, 2010), and other geomorphic processes (Stoffel and Corona, 2014). In dendrogeomorphic studies, 200 the primary unit of analysis is growth disturbances (GDs) in the tree-ring record, which reflect external stresses experienced by the tree. These are often expressed as a decrease in springwood width (the lighter portion of the growth ring) compared to the springwood of adjacent annual rings.

We used high-resolution images from Google Earth and Landsat 8 OLI to identify areas of high likelihood of GD. Similar to 205 the sediment samples, we identified potential sampling sites based on several expert informed sampling strategies, summarized in table 2.

Table 2. Dendrogeomorphologic Sample Extraction Characteristics

Characteristic	Underlying Logic
Immediately adjacent to Rio Soler	These areas would receive the initial forces of the flood wave, increasing likelihood of GD.
Prioritized stands of trees that with front row running perpendicular to valley	Front row of trees would likely experience higher forces of flood waters, increasing chances of scarring, remnant debris, and GD.

Originally, the research plan was to identify visible scarring which would be used to sample the date of scarring (Ballesteros- 210 Cánovas et al., 2015; Gorsic et al., 2025), yet a lack of prominent and identifiable visible scarring required a change of strategy to statistically relate GDs in tree ring thicknesses. We opted to find trees that would have been impacted by stressors such as the impact wave, damage from passing debris, or other geomorphologic changes that would have induced stress for the growing 215 conditions of the tree. We collected n=50 samples from the several species of the *Nothofagus* genus (Southern Beech), including *N. pumilio* (Lenga), *N. betuloides* (Coihue), and *N. dombeyi* (Ñirre). Although these species have been effectively used in dendrochronological studies in Patagonia (Gorsic et al., 2025; Winchester & Harrison, 2000), their application to 220 assessing impacts from GLOF events remains limited. We collected samples from trees with a diameter between 15 - 35 cm. Where possible, we identified trees that had visible scars on their stem surface, which we interpreted as reflecting impact of passing debris from the 1989 flood event.

Samples were analyzed and processed following standard procedure (Bollschweiler et al., 2008; Stoffel and Corona, 2014). Samples were mounted on a slotted mount and prepared with a fine grit sand-paper size 600 that allowed for ring identification. 225 Using the CooRecorder 9.0 software (Larsson, 2013), we counted tree-rings and measured widths from high-resolution (1200 dpi) digitized images, and transferred output files into COFECHA (Richard L. Holmes, 1983) for cross-dating analysis.

2.7 Carbon-14 Dating

We collected two samples (n = 2) of buried vegetation from downstream deposits to radiocarbon date a previously undocumented GLOF event which emanated from Laguna Turbio (figure 1) and whose geomorphologic impacts are visible in 225 historic remote sensing imagery. Using the RPA, we recovered two distinct organic layers from a stratigraphically continuous sequence, each representing a buried vegetation horizon. Our objective was to correlate the shallower (and therefore younger)



sample with the known 1989 GLOF, thereby inferring that the deeper layer may correspond to an earlier, unrecorded event. If validated, this organic layer would give an approximate date for the previously undocumented GLOF originating from Laguna Turbio. The two samples were processed as bulk carbon and analyzed in the University of Colorado Boulder AMS Radiocarbon 230 Prep Laboratory. While this is not a statistically robust sampling of the sedimentary deposits, further assessment of ^{14}C dates was unfeasible due to the cost of testing.

3 Results

The 1989 GLOF transported an estimated $9.5 \times 10^6 \text{ m}^3$ of sediment from the burst moraine (Burton et al., 2020). Coarser sediments accumulated in the upper reaches of Valle Soler near the breached moraine, while deposition of finer sediment 235 extended throughout the valley's lower stretches. Sediment grain sizes exhibit sharp gradations with increasing distance from the failed moraine, consistent of high-energy outburst flood deposits transitioning into lower-energy depositional environments (Sincavage et al., 2023).

3.1 Witness Accounts of the Flood

We used witness accounts of the flood to constrain key parameters used as model input (full interviews are found in S1), using 240 their locations and descriptions of flood behavior. According to those that witnessed the event, there were only four people in the valley when the flood occurred, of which only three are surviving. I spoke with all three of the surviving witnesses to reconstruct the flood using the hydrologic models. From the interviews, we gathered important discrepancies from descriptions of the previous scientific accounts. Firstly, two brothers and a third helper were working in the upper section of Valle Soler when they saw the rushing wave of water. They describe a rapidly descending flurry of water that filled from valley wall to 245 valley wall (cordillera a cordillera). One worker had to rapidly climb a tree, some 6-8 meters high to avoid being swept away, and the brothers scrambled up a nearby hill.

These accounts contrast dramatically with the hydrologic model results of peak discharge estimates by Hauser (1993) which calculated, from empirical relations, the discharge to be around $2000 \text{ m}^3\text{s}^{-1}$. Modeled results with Hauser's peak discharge were insufficient to replicate the magnitude and depth of flooding witnessed (Burton et al., 2020). Secondarily, the mode of 250 moraine failure varied from accounts. From the initial report, Hauser posits an iceberg likely blocked the outlet causing the eventual failure of the dam, either from overtopping or compromising the dam as the water moved around the blockage. This differs from the witness accounts, all of whom did not mention an eventual increase of flood waters but describe the advancing flood wave as "all-at-once", leaving them with little time to escape. Two witnesses stated they thought the moraine must have failed from below to release so much of its waters so rapidly.

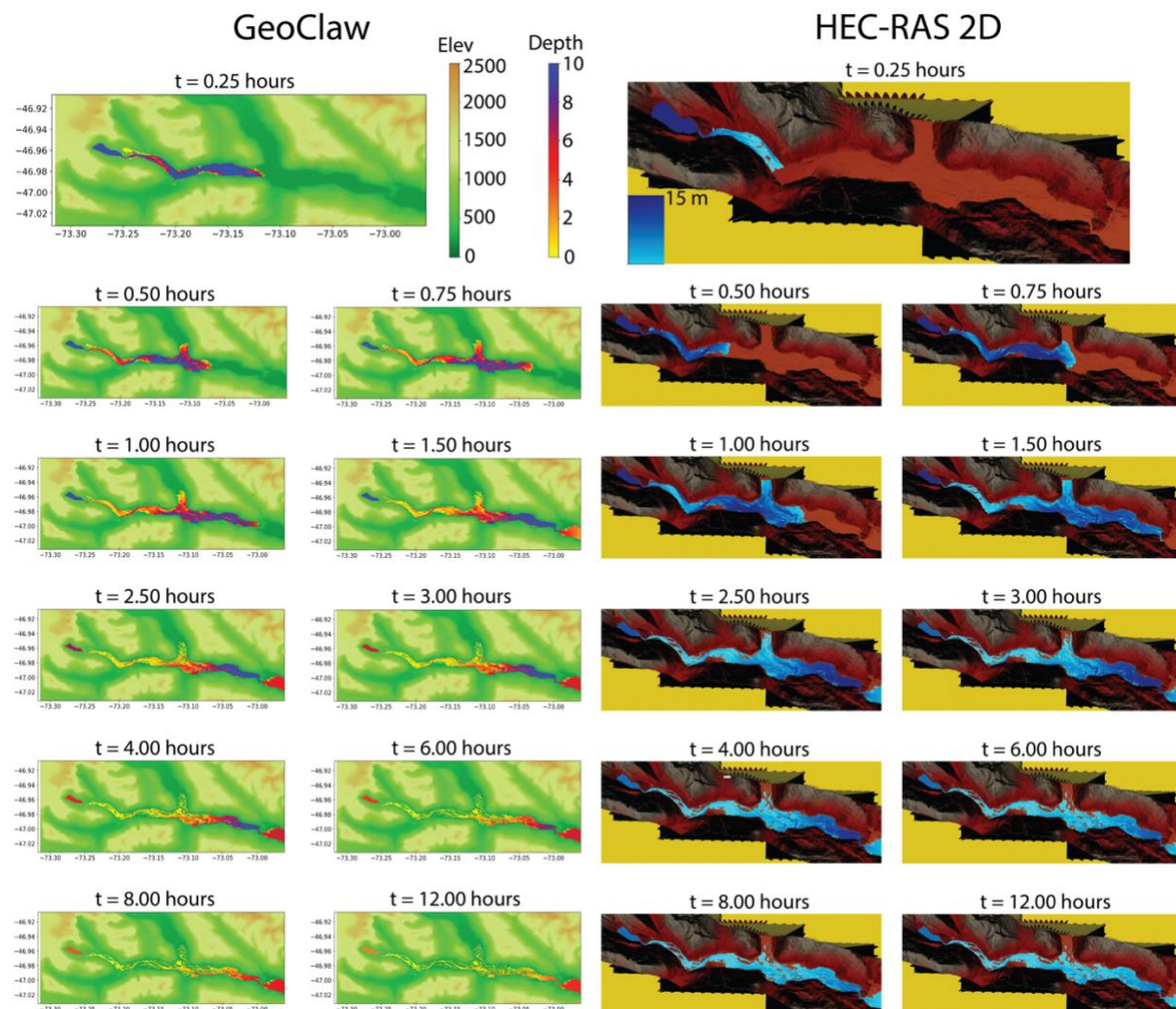
255 Further downstream, the third witness describes his account of the flood, when he went out of the small barn to attend to horses that had been scared by something. From there, he describes a wave of water that washed over a coigue (6-8 m tall). He jumped



on a mare and started climbing, narrowly escaping the oncoming flood wave. So narrowly, in fact, that he was hit in the back by a tree carried by the wave which left him with a discernible limp for the rest of his life.

3.2 Hydrologic Models

260 Hydrologic model outputs of the 1989 event largely coincide between the two approaches, yet important differences arise based on the different initial assumptions (Figure 4, videos S2). As noted by Turzewski et al. (2019), the assumption from GeoCLAW of instantaneous dam failure leads to higher peak discharges and shorter time to peak discharge than would be otherwise be expected. This is evident through an apparent 15-30 minute advance in the GeoCLAW simulation compared with HEC-RAS 2D at the same Δt .



265

Figure 4. Comparison of simulated flood wave progression from GeoClaw and HEC-RAS 2D models as a function of time since breach initiation (Δt). The GeoClaw model shows a lag in wavefront propagation relative to the HEC-RAS 2D results.

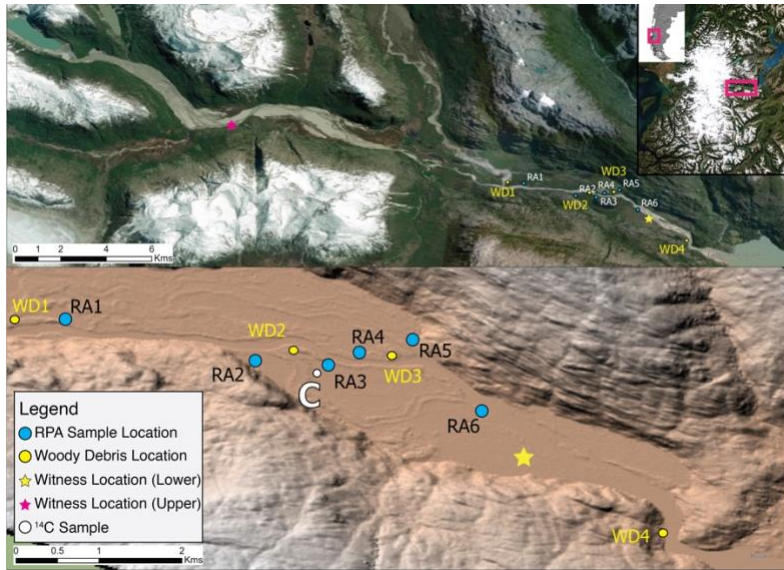


The GeoCLAW simulation fully floods the downstream valley filling the canyon walls with 10m of water, reaching the Rio Cacho tributary (Figure 1) within the first 15 minutes. The flood, upon reaching the wider stretches of the middle Valle Soler, 270 attenuates a portion of the energy and advancing flood wave height to 4-6 meters. A portion of the flood is diverted north, moving upstream of Rio Cacho. Within only 60 minutes, the wave front has nearly reached the end of the valley while the main bulk of water volume accumulates into a trailing pulse of water growing and diminishing in height with the contours and constrictions of the valley walls. By the end of the first hour, the bulk volume of the flood reaches the furthest stretches of Valle Soler, where an end moraine creates an abrupt constriction with two near 90° diversions that causes the water to pool 10 275 meters deep as it moves through the constriction and drains into Lago Plomo.

HEC-RAS 2D, by contrast, includes a dam-break module that allows users to define initial conditions replicating the physical characteristics of a dam. In this case, the gradual erosion of the terminal moraine moderates the downstream propagation and reduces the depth of the advancing flood wave (Figure 4). The simulation initiates with shallow overtopping that begins 280 flooding the upper section of Valle Soler, followed by the main flood wave breaching the moraine and overtaking the initial inundation front. Notably, there is a time lag of approximately 30 minutes in the arrival of the bulk flood pulse in the HEC-RAS simulation compared to GeoCLAW for comparable downstream locations. The bulk flood pulse similarly reaches depths exceeding 10 meters, dependent on the constrictions of the valley width, accumulating at the final constriction at 90 minutes. The bulk flood pulse pools at this constriction for some 3-4 hours as the outlet slowly drains the flood water into Lago Plomo.

3.3 Sediment Samples

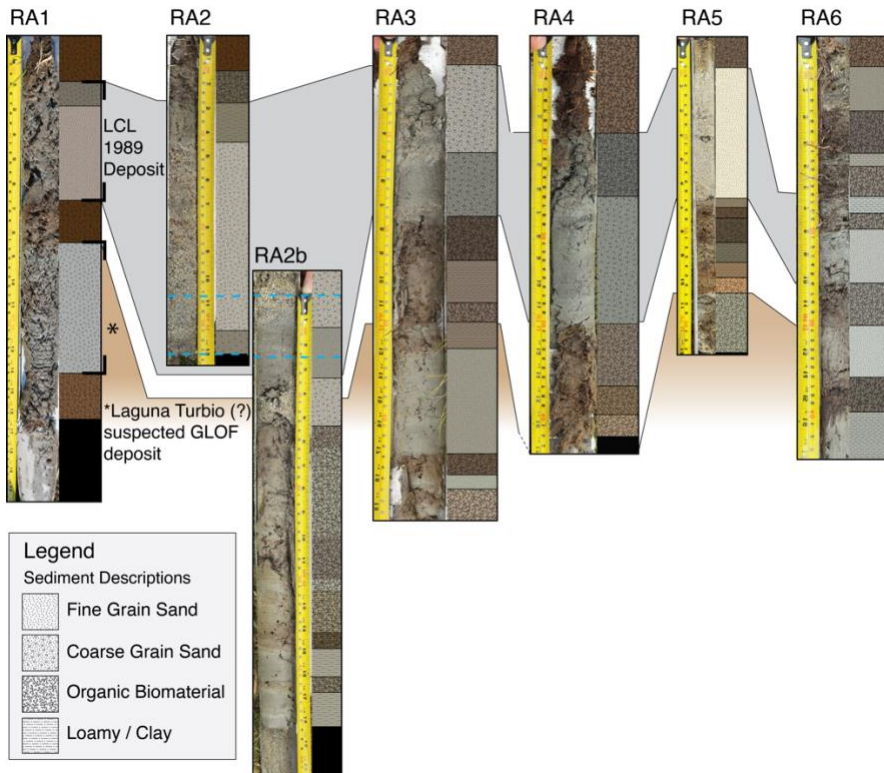
285 The sediment deposited by the 1989 Soler GLOF displayed a range of depositional environments (Figure 5), indicative of the changing downstream hydrologic impacts of glacial recession (Milner et al., 2017). Sediment ranged from silt/clay sized particles to coarse (phi scale $d=1.0$) sand, interspersed with organic horizons. When extracting sediment samples, we interpreted the first non-organic lens of clastic sediment to be most likely deposited by the 1989 GLOF, informed by campesino's accounts that Rio Soler had not flooded its banks since the 1989 GLOF. This depositional layer varied in sediment 290 size and thickness throughout the valley but was consistently present in the extracted samples. The organic horizons similarly varied in thickness, which we interpreted to the various geomorphologic environments in which they were found (i.e., low-lying wetland, seasonal pasture, raised floodplain). In many, but not all samples, we observed a repeated pattern of organic horizon, clastic lens, organic horizon, clastic lens, which we interpreted as a GLOF depositional layer from the prior (Laguna Turbio) GLOF.



295

Figure 5. Map of the samples collected in the lower stretches of Valle Soler. The blue dots represent sediment cores extracted by the Russian Peat Auger. The yellow dots represent woody debris found in the field. The stars indicate the location of the campesinos when the flood occurred. The white 'C' symbol represents where the carbon sample was extracted for ¹⁴Carbon dating. Powered by Esri.

300 In all, we collected six sediment samples using the RPA (S3), and another nine using the sediment probe (Figure 6). At each site, we typically extracted two pilot probes using the sediment probe to gain a snapshot of the substrata, but a malfunction with the rotating blade on the RPA inhibited further use at several locations, as the sediment was either too dry (would crumble apart) or over saturated with water (and would not hold its shape once extracted).



305 **Figure 6. Lithology of extracted sediment cores RA1-6.** Sediment was extracted using an RPA in the floodplain of Valle Soler. Sediments deposited from the 1989 GLOF (grey) are present in each of the extracted cores, characterized by coarse, silica-rich sand with an organic horizon above and below the deposited sediment. In four cores a similar sediment stratum (*light brown) is present below the 1989 deposition and is believed to have originated from a GLOF from the Laguna Turbio basin. ^{14}C dating revealed this GLOF took place late 19th / early 20th C. Detailed descriptions of the sediment lithology found in S3.

310 3.4 Dendro-geomorphologic impacts

A total of 50 cores were extracted from *N. pumilio* (Lenga, n= 34), *N. betuloides* (Coihue, n=10), and *N. dombeyi* (Ñirre, n=6). Where several studies have successfully related growth disturbances of trees with geomorphological processes such as flash floods (Casteller et al., 2015) and debris flows (Bollschweiler and Stoffel, 2010), few studies have related dendrogeomorphic samples with GLOFS (Gorsic et al., 2025), and this is still a developing science. In the field, we found many trees to have a 315 strong outer bark, but to be soft and rotten on the inside beyond a few centimeters (~ 6 – 10 cm). We later found out that *Nothofagus* species are impacted by a spreading fungus which produces similar symptoms of inner rot, particularly in wetter environments (Cwielong and Rajchenberg, 1995) that significantly inhibited a more robust sampling for dendrogeomorphic impacts. Indeed, upon subsequent analysis, we found fourteen of the samples to be partially rotten to such a degree that we were unable to extract reliable ring counts from them and had to be discarded. Seven samples from these 320 did not reach the desired temporal extent to capture the 1989 event and were similarly unusable. From the remaining n=29 samples, we were only able to obtain a series intercorrelation of .343 convergence on the tree ring growth disturbances. For this reason, we opted to abandon the dendrogeomorphic data (S4).



325 There was a surprising lack of evidence of the relatively recent 1989 GLOF in the downstream reaches, raising further questions about the longevity of geomorphologic impacts of GLOFs in Patagonia (Emmer, 2023b). We found several sites of accumulated woody debris of such a magnitude that we strongly suspected was deposited from the 1989 GLOF (Fig 7). The large trunks were uniformly decayed and piled several meters above the current Rio Soler high water bank, indicating that the accumulated trees had been there for some time (decades) and were not likely to have been deposited from normal seasonal high flow.



330 **Figure 7. Dendrogeomorphic impacts from the 1989 GLOF.** Images A and B indicate scarring found on the river-facing aspect of two large *Nothofagus Pumilio* (Lenga) trees. Images A-C were captured at WD1. Image D (WD3) shows a remnant log that was likely stranded in the canopy of another tree, given the advanced state of decomposition which matched other accumulations of woody debris. Image E was taken at WD4, likely caught as the leading wave front passed through the topographic bottleneck.

335 Some older living trees retained large scars on the upstream side of their trunk, likely sustained by the initial impact of the debris-laden flood wave. However, we were unable to extract dendrogeomorphic samples from these scarred trees; those trees that we were able to find with scarring were either rotten from the fungus described previously or were sufficiently large that our tree corers were not able to enter deep enough into the tree to extract the respective growth ring.

340 Finally, the topographical constriction in the lower valley caused floodwaters to temporarily pool before being funneled through the narrow channel toward Lago Plomo. A prominent eddy bar deposit (Figure 8) situated approximately 8-12 meters above Río Soler, was likely deposited as the impounded water drained into Lago Plomo.



Figure 8. Flood eddy deposit observed on the outlet of the constriction (opaque red). This was likely deposited during the backwater accumulation of water, as it drained from the topographic constriction near the outlet of the river into Lago Plomo (river flow direction is left to right).

345 3.5 Carbon-14 Dating of Laguna Turbio GLOF

Clear geomorphic indicators of the 1989 flood are still present in the valley. However, these same features complicate the interpretation of additional evidence pointing to an earlier GLOF event that also impacted the landscape. For example, an analysis of sediment transportation during the 1989 event showed a counterintuitive coarsening of grainsize, before a gradual fining (Sincavage et al., 2023). While planning for the field expedition, remote sensing analysis suggested a prior outburst 350 flood originating from the adjacent Laguna Turbio (Figure 1). Field observations supported this hypothesis, revealing multiple indicators of a past GLOF: a breached terminal moraine, a visibly lowered lake level, a downstream impact zone, and a consistent reduction in tree size across the suspected flood path—suggestive of uniform re-colonization following disturbance (Emmer, 2023).

We extracted and analyzed organic material from sediment samples from the RPA to date the deposition of clastic sediment 355 on top of the vegetation layer that we assumed as preexisting peat vegetation present before the 1989 GLOF. The ^{14}C sample taken from the layer expected to have originated returned “modern age”, with a fractional carbon at 1.1921 (Figure 9). This indicates a high likelihood that our collected ^{14}C sample was taken from organic material deposited in the 1989 flood. The second ^{14}C sample measured a final fractional carbon ratio of 0.9845, with an estimated age of 125 ybp (std 20). From the time of analysis (2024), which would mean the GLOF event took place in 1899 ± 20 years.

360

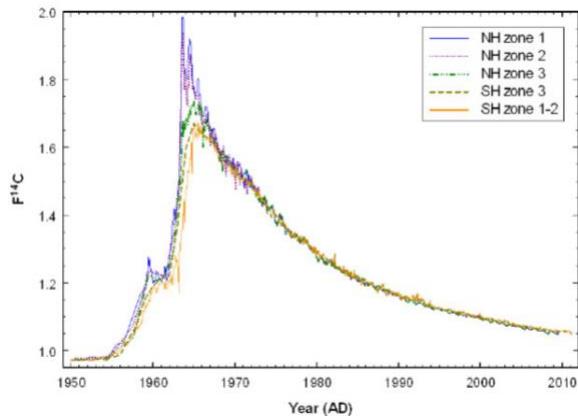


Figure 9. From Hua et al., (2013). Compiled (extended) monthly atmospheric Fractional ^{14}C curves for 5 different zones (NH zone 1, NH zone 2, NH zone 3, SH zone 3, and SH zone 1-2). Chile is within SH zone 2 (orange solid).

4 Discussion

365 4.1 Initial Conditions and Flood Dynamics

The end moraine that dams LCL was breached by a large volume of water, approx. $140 \times 10^6 \text{ m}^3$ (Burton et al., 2020) that rapidly incised through the moraine sediment. Witnesses did not observe a gradual onset of flood waters that would have signaled an impending flood, rather, they describe the main flood surge quickly overtook the initial wave front, with the advancing flood wave likely reaching several meters in height. The rapid advancement of the flood wave is corroborated by 370 both hydrologic models, as well as witness testimony.

The original report on this event prescribes the flood trigger was due to an iceberg that clogged the drainage, causing the lake to overflow and begin morainal incision. We find this conclusion unlikely due to the rapidity of the rate of breach formation. Given that the flood occurred late in the austral summer and the upper cirque headwall lacked an ice apron, we consider it more likely that a large icefall generated an overtopping wave that catastrophically breached the moraine dam.

375 GLOFs are characterized by their high sediment entrainment capacity and erosive/depositional potential (Emmer, 2023a; Richardson and Reynolds, 2000; Turzewski et al., 2019). These characteristics also are strongly modulated by geographic controls like downstream valley slope angle and topographic terrain (Clague and Evans, 2000; O'Connor and Costa, 1993; Westoby et al., 2014), and may fluctuate between flow regimes depending on available sediment or changes in slope (Clague et al., 1985; Evans, 1986; Hungr et al., 1984). The Soler GLOF mobilized very large boulders (Figure 10, spanning 3 - >8 380 meters) and likely initially behaved more like the dense slurry of a debris flow. However, this flood likely rapidly attenuated in initial 12 kms, as several abrupt turns, valley widenings, and a shallow slope angle allowed the flood waters to spread laterally, decreasing the turbidity of the outburst flood. Sediment redistribution did continue downstream, but to much less of an effect than in the upper reaches of the valley. Witnesses recounted how everything was left in a coating of white ultra-fine glacial flour following the flood, but that the glacial flour washed away after subsequent precipitation.

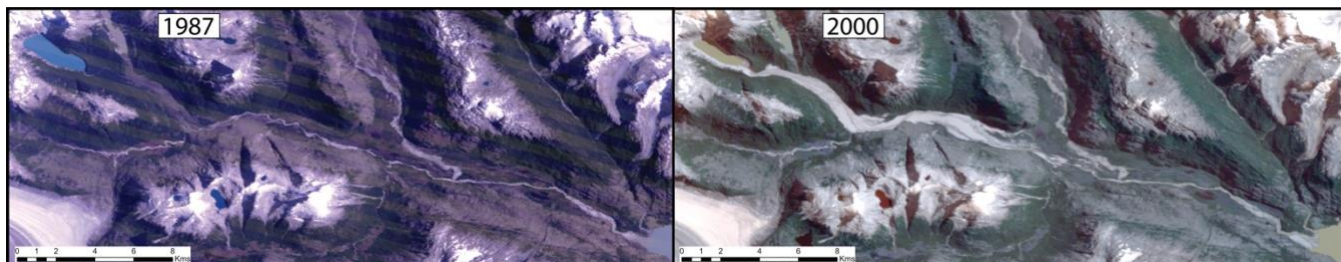


385

Figure 10. Image of boulders mobilized by the 1989 GLOF in the upper Soler Valley, some of them measuring over 8m (Photo taken by Cris Enriquez).

4.2 (Mis)Reading the Landscape

The lack of easily accessible and decipherable evidences of previous GLOF impacts in the lower reaches of Valle Soler raises
390 important questions regarding the legibility of GLOF indicators, similarly analyzed by Emmer (2023b). Beyond the initial
sediment redistribution of upper Soler, the lower portions of the valley remained seemingly undisturbed, with less
geomorphological impacts visible from available remote sensing (Figure 11). Moreover, compounding GLOF events, such as
occurred with LCL and Laguna Turbio, further complicate the legibility of even large-magnitude GLOF events.



395 **Figure 11. Historic imagery Landsat 5 (TM) of Valle Soler. Valle Soler deposits are clearly visible in the post-GLOF (2000) image, and similar impacts are visible emanating from Laguna Turbio.**

Conventional methodological approaches to estimating peak discharge in GLOF events can significantly misrepresent the true
magnitude of these extreme events, particularly when applied beyond the empirical range of their original datasets. In this
400 case, the initial empirical equations used by Hauser (1993) to estimate peak discharge (Q_p) underestimated the flood by nearly
an order of magnitude. This discrepancy likely stems from the unusually large volume of Laguna Cerro Largo (LCL), which
exceeds the scale of events used to derive those equations. The formula that was applied in the official report relates discharge
(Q_p) to the volume of water drained, yet the case studies collated into this database were collected from ice-dammed lakes
(Clague and Mathews, 1973), skewing the results in the 1989 Soler GLOF. Other formulae, like Costa and Schuster (1988)
405 were based on data linking Q_p to the calculated potential energy of the impounded lake. Those data points ranged from
approximately 10^{10} to 10^{12} joules, whereas calculations with data taken from Burton et al. (2020) suggest a potential energy
closer to 10^{14} joules—two orders of magnitude greater.



The limitations of empirical formulae become more evident when compared to eyewitness testimony. All accounts, given by individuals located at different points in the valley, consistently describe a sudden onset of a high-energy, torrential flow that stood several meters tall. Witnesses reported that the floodwaters rapidly inundated the entire valley floor, reaching depths of 410 several meters at their respective locations. These descriptions sharply contrast with Hauser's estimated peak discharge (Q_p) of 1800 - 2000 cubic meters per second. At that rate, and assuming sustained peak flow, it would have taken approximately 31 hours to drain his estimated flood volume of 229×10^6 cubic meters (Hauser, 1993). In contrast, interviewees recalled that the bulk of the flood passed through in just 8 hours—long enough for one campesino to spend the night in a tree, which he had climbed 6 to 8 meters above the ground to escape the rising waters. This discrepancy suggests that the original discharge 415 estimate significantly underestimated the true magnitude of the event.

While these empirical equations have been reanalyzed and calibrated in the decades since, it is important to note that the applied results of these formulae often are not, with lasting consequences for policy and hazard planning. Local policymakers and scientists were more familiar with estimates in the 2000-3000 m³ range, citing Hauser (1993) and the cyclical ice-dammed 420 GLOFs from Cachet II (Jacquet et al., 2017). Discrepancies like these comprise a potentially dangerous miscommunication that impact subsequent development of policy and emergency preparedness plans.

4.3 Epistemological Blind Spots and Interdisciplinary Approaches

GLOFs have been studied predominately from glaciological and other Earth science perspectives. While contributing a foundational geophysical understanding of the complex process chains and downstream impacts, the remote nature of these processes complicates analysis where data is often sparse or non-existent. As illustrated by Williams et al. (2022), triangulating 425 an understanding of geomorphic events such as GLOFs using diverse data can help reconstruct geomorphic processes in data sparse areas.

The 1989 Soler GLOF is readily identifiable in satellite imagery, with distinct geomorphic signatures detectable via remote sensing. However, the temporal resolution is constrained by the infrequent revisit times of early satellite platforms at mid-latitudes and by persistent cloud cover, customary for this region. Additionally, repeat events, such as the overlaid GLOF 430 deposition from the Soler and Turbio GLOFs, obscure the prior events and their visible indicators.

Witness testimonies were integral to providing crucial data for the hydrologic models. Further, their local expertise and intimate familiarity with the landscape provided additional details that would be otherwise exceedingly difficult to extract via remote sensing. For example, the dense vegetation present in the valley has all but obscured the most obvious of geomorphologic features of the outburst flood. Moreover, local familiarity with the land is an underappreciated source of knowledge in scientific 435 research (Balay-As et al., 2018; Cadag and Gaillard, 2012). Campesino accounts of a rapid and catastrophic moraine dam failure aligned more closely with the results of the hydrologic simulation than with the moderated descriptions and initial reports. Community members also demonstrated awareness of other potentially hazardous moraine-dammed lakes within the valley. Yet these histories were seemingly underappreciated from the initial surveys, as the official report contain only fleeting references to witness testimonies in passing (Hauser, 1993).



440 This research illustrates an important first step in approaching a more holistic understanding of GLOF risks, similar to other
441 mixed-methods reconstruction of flood events (Williams et al., 2022). Given the limited empirical data and uncertain dynamics
442 of glacier-lake systems in the region, establishing how, when, and where floods occur is a crucial first step in contextualizing
443 the lived, political, and governance dimensions of hazard. These findings therefore give an essential—if partial—contribution
444 toward a more holistic understanding of GLOF risk that integrates material processes with the social and institutional
445 conditions through which risk is produced and experienced.

However, there are also many challenges and limitations that arise from this type of work. The inability to statistically correlate samples taken from impacted trees, despite this methodology being successfully applied in similar contexts (Gorsic et al., 2025) underlines the difficulty of interdisciplinary research. Reconstructing extreme events through hydrologic modeling require extensive and accurate input data, and may inherently contain uncertainty (Westoby et al., 2014; Williams et al., 2022).

450 For example, the peak discharge reported here is likely an overestimate, reflecting the underlying assumptions and simplifications of the hydrologic model. As with empirical formulas that require context-specific calibration, it is important to acknowledge that scientific results often take on a political life of their own that may persist unexamined long after the initial analysis is complete.

5 Conclusion

455 This research reconstructs the geomorphic and hydrologic impacts of a glacial lake outburst flood originating from Laguna del Cerro Largo, and integrates field-based observations, sedimentological analysis, and two-dimensional hydraulic modeling with witness accounts in order to analyze gaps existing between the impacts experienced by locals and official reports of the event. There are inherent limitations in reconstructing past events due to availability of data, assumptions embedded within hydrologic models, and the rarity and magnitude of the processes entailed. The official report underestimated the severity and 460 downstream impacts of the event. Decades later, the scientific output of that report continues to shape the political landscape of disaster planning and policy. In contrast, campesino testimonies aligned more closely with the hydrologic reconstructions and drew attention to other potentially unstable lakes in the valley, suggesting a deeper, place-based awareness of glacial hazards. This approach highlights the critical insights that local engagement brings to the scientific study of landscape change and hazards.

465 This case study contributes to the growing body of literature on GLOF processes in Patagonia, providing empirical constraints on the sedimentary and hydrologic dynamics of moraine-dam failures in glaciated catchments. Moreover, it offers a replicable methodological framework for reconstructing undocumented or poorly monitored GLOF events in similarly remote or data-scarce environments, underlining the strengths of community-engaged science.

Author contribution: Jonathan Burton designed and conducted the research, with input from Frederick Chambers and Lisa 470 Kelley. Jonathan also prepared the manuscript with contributions from all authors. Benjamin Soto Narbona assisted in the field portion and data analysis of the dendrogeomorphologic samples.



Conflict of Interest: The authors declare that they have no conflict of interest.

Acknowledgments: We would like to thank Waldo Aguayo Riquelme for guiding the field work and logistical support, as well as the interview respondents for providing their accounts. Thank you Randy LeVeque and David George for their generous 475 support in running the GeoClaw model. We would also like to thank the communities of Puerto Bertrand and Cochrane for their hospitality.

References

Allen, S., Frey, H., and Huggel, C.: GAPHAZ 2017: Assessment of Glacier and Permafrost Hazards in Mountain Regions. Technical Guidance Document, Standing Group on Glacier and Permafrost Hazards in Mountains (GAPHAZ) of the 480 International Association of Cryospheric Sciences (IACS) and the International Permafrost Association (IPA), Switzerland / Lima, Peru, 2017.

Balay-As, M., Marlowe, J., and Gaillard, J. C.: Deconstructing the binary between indigenous and scientific knowledge in disaster risk reduction: Approaches to high impact weather hazards, *International Journal of Disaster Risk Reduction*, 30, 18–24, <https://doi.org/10.1016/j.ijdrr.2018.03.013>, 2018.

485 Ballesteros-Cánovas, J. A., Stoffel, M., St George, S., and Hirschboeck, K.: A review of flood records from tree rings, *Progress in Physical Geography: Earth and Environment*, 39, 794–816, <https://doi.org/10.1177/0309133315608758>, 2015.

Blair, H., Bosak, K., and Gale, T.: Protected Areas, Tourism, and Rural Transition in Aysén, Chile, *Sustainability*, 11, 7087, <https://doi.org/10.3390/su11247087>, 2019.

490 Bollschweiler, M. and Stoffel, M.: Tree rings and debris flows: Recent developments, future directions, *Progress in Physical Geography: Earth and Environment*, 34, 625–645, <https://doi.org/10.1177/0309133310370283>, 2010.

Bollschweiler, M., Stoffel, M., and Schneuwly, D. M.: Dynamics in debris-flow activity on a forested cone — A case study using different dendroecological approaches, *CATENA*, 72, 67–78, <https://doi.org/10.1016/j.catena.2007.04.004>, 2008.

495 Burton, J. W., Chambers, F. B., Sincavage, R., and Cross, M. D.: Analysis of Glacial Lake Outburst Flood Terrain Sedimentary Deposits in Valle Soler, Northern Patagonian Icefield, *Physical Geography*, 43, 333–349, <https://doi.org/10.1080/02723646.2020.1839213>, 2020.

Cadag, J. R. D. and Gaillard, J.: Integrating knowledge and actions in disaster risk reduction: the contribution of participatory mapping, *Area*, 44, 100–109, <https://doi.org/10.1111/j.1475-4762.2011.01065.x>, 2012.

500 Carrivick, J. L., Davies, M., Wilson, R., Davies, B. J., Gribbin, T., King, O., Rabatel, A., García, J., and Ely, J. C.: Accelerating Glacier Area Loss Across the Andes Since the Little Ice Age, *Geophysical Research Letters*, 51, e2024GL109154, <https://doi.org/10.1029/2024GL109154>, 2024.

Casteller, A., Stoffel, M., Crespo, S., Villalba, R., Corona, C., and Bianchi, E.: Dendrogeomorphic reconstruction of flash floods in the Patagonian Andes, *Geomorphology*, 228, 116–123, <https://doi.org/10.1016/j.geomorph.2014.08.022>, 2015.

505 Clague, J. J. and Evans, S. G.: A review of catastrophic drainage of moraine-dammed lakes in British Columbia . Quaternary Science Reviews A review of catastrophic drainage of moraine-dammed lakes in British Columbia, *Quaternary Science Reviews*, 19, 1763–1783, [https://doi.org/10.1016/S0277-3791\(00\)00090-1](https://doi.org/10.1016/S0277-3791(00)00090-1), 2000.



Clague, J. J., Evans, S. G., and Blown, I. G.: A debris flow triggered by the breaching of a moraine-dammed lake, Klattasine Creek, British Columbia, *Can. J. Earth Sci.*, 22, 1492–1502, <https://doi.org/10.1139/e85-155>, 1985.

Cwielong, P. P. and Rajchenberg, M.: Wood-rotting fungi on *Nothofagus pumilio* in Patagonia, Argentina, *European Journal of Forest Pathology*, 25, 47–60, <https://doi.org/10.1111/j.1439-0329.1995.tb01071.x>, 1995.

510 Dussaillant, A., Benito, G., Buytaert, W., Carling, P., Meier, C., and Espinoza, F.: Repeated glacial-lake outburst floods in Patagonia: An increasing hazard?, *Natural Hazards*, 54, 469–481, <https://doi.org/10.1007/s11069-009-9479-8>, 2010.

Dussaillant, I., Berthier, E., and Brun, F.: Geodetic Mass Balance of the Northern Patagonian Icefield from 2000 to 2012 Using Two Independent Methods, *Frontiers in Earth Science*, 6, 1–13, <https://doi.org/10.3389/feart.2018.00008>, 2018.

515 Dussaillant, I., Berthier, E., Brun, F., Masiokas, M. H., Hugonnet, R., Favier, V., Rabatel, A., Pitte, P., and Ruiz, L.: Two decades of glacier mass loss along the Andes, *Nature Geoscience*, 12, 802–808, 2019.

Emmer, A.: Geomorphological Imprints of Major Glacial Lake Outburst Floods (GLOFs): First Insights from Peru-wide GLOF Inventory, *Revista de Glaciares y Ecosistemas de Montaña*, 8, 77–87, 2023a.

Emmer, A.: Vanishing evidence? On the longevity of geomorphic GLOF diagnostic features in the Tropical Andes, *Geomorphology*, 422, 108552, <https://doi.org/10.1016/j.geomorph.2022.108552>, 2023b.

520 Evans, S. G.: The maximum discharge of outburst floods caused by the breaching of manmade and natural dams., *Canadian Geotechnical Journal*, 23, 1986.

Froehlich, D. C.: PEAK OUTFLOW FROM BREACHED EMBANKMENT DAM, *Journal of Water Resources Planning and Management*, 121, 90–97, 1995.

525 Gorsic, S., Corona, C., Manchado, A. M.-T., Lopez-Saez, J., Allen, S., Ballesteros-Cánovas, J. A., Dussaillant, A., and Stoffel, M.: Coupling tree-ring and geomorphic analyses to reconstruct the 1950s massive Glacier Lake Outburst Flood at Grosse Glacier, Chilean Patagonia, *Science of The Total Environment*, 961, 178368, <https://doi.org/10.1016/j.scitotenv.2025.178368>, 2025.

Hauser, A.: Remociones en masa en Chile, edited by: *Boletín 59*, Servicio Nacional de Geología y Minería, Santiago, 89 pp., 1993.

530 Hock, R., Rasul, G., Adler, C., Cáceres, B., Gruber, S., Hirabayashi, Y., Jackson, M., Kääb, A., Kang, S., Kutuzov, S., Milner, A., Molau, U., Morin, S., Orlove, B., and Steltzer, H.: High Mountain Areas, [H.-O. Pörtner, D.C. Roberts, V. Masson-Delmotte, P. Zhai, M. Tignor, E. Poloczanska, K. Mintenbeck, A. Alegría, M. Nicolai, A. Okem, J. Petzold, B. Rama, N.M. Weyer (eds.)], Cambridge University Press, Cambridge, UK and New York, NY, USA, 2019.

535 Hugonnet, R., McNabb, R., Berthier, E., Menounos, B., Nuth, C., Girod, L., Farinotti, D., Huss, M., Dussaillant, I., Brun, F., and Kääb, A.: Accelerated global glacier mass loss in the early twenty-first century, *Nature*, 592, 726–731, <https://doi.org/10.1038/s41586-021-03436-z>, 2021.

Hungr, O., Morgan, G. C., and Kellerhals, R.: Quantitative analysis of debris torrent hazards for design of remedial measures, *Can. Geotech. J.*, 21, 663–677, <https://doi.org/10.1139/t84-073>, 1984.

IPG: *Inventario Público de Glaciares*, Dirección General de Aguas, 2022.



540 Iribarren Anacona, P., Mackintosh, A., and Norton, K.: Reconstruction of a glacial lake outburst flood (GLOF) in the Engaño valley, chilean patagonia: Lessons for GLOF risk management, *Science of the Total Environment*, 527–528, 1–11, <https://doi.org/10.1016/j.scitotenv.2015.04.096>, 2015.

545 Iribarren Anacona, P., Sepúlveda, C., Berkhoff, J., Rojas, I., Zingaretti, V., Mao, L., Mazzorana, B., and Durán, G.: Cascading Impacts of GLOFs in Fluvial Systems: The Laguna Espontánea GLOF in Patagonia, in: *Rivers of Southern Chile and Patagonia: Context, Cascade Process, Geomorphic Evolution, and Risk Management*, edited by: Oyarzún, C., Mazzorana, B., Iribarren Anacona, P., and Iroumé, A., Springer International Publishing, Cham, 2023.

Jacquet, J., McCoy, S. W., McGrath, D., Nimick, D. A., Fahey, M., O'kuinghtons, J., Friesen, B. A., and Leidich, J.: Hydrologic and geomorphic changes resulting from episodic glacial lake outburst floods: Rio Colonia, Patagonia, Chile, *Geophysical Research Letters*, 44, 854–864, <https://doi.org/10.1002/2016GL071374>, 2017.

550 Klimeš, J., Benešová, M., Vilímek, V., Bouška, P., and Cochachin Rapre, A.: The reconstruction of a glacial lake outburst flood using HEC-RAS and its significance for future hazard assessments: An example from Lake 513 in the Cordillera Blanca, Peru, *Natural Hazards*, 71, 1617–1638, <https://doi.org/10.1007/s11069-013-0968-4>, 2014.

555 Kougkoulos, I., Cook, S. J., Edwards, L. A., Clarke, L. J., Symeonakis, E., Dortch, J. M., and Nesbitt, K.: Modelling glacial lake outburst flood impacts in the Bolivian Andes, *Nat Hazards*, 94, 1415–1438, <https://doi.org/10.1007/s11069-018-3486-6>, 2018.

Larsson, L.: CooRecorder and Cdendro programs of the CooRecorder/Cdendro package, 2013.

Lützow, N., Veh, G., and Korup, O.: A global database of historic glacier lake outburst floods, *ESSD – Land/Hydrology*, <https://doi.org/10.5194/essd-2022-449>, 2023.

560 Milner, A. M., Khamis, K., Battin, T. J., Brittain, J. E., Barrand, N. E., Füreder, L., Cauvy-Fraunié, S., Gíslason, G. M., Jacobsen, D., Hannah, D. M., Hodson, A. J., Hood, E., Lencioni, V., Ólafsson, J. S., Robinson, C. T., Tranter, M., and Brown, L. E.: Glacier shrinkage driving global changes in downstream systems, *Proc. Natl. Acad. Sci. U.S.A.*, 114, 9770–9778, <https://doi.org/10.1073/pnas.1619807114>, 2017.

O'Connor, J. E. and Costa, J. E.: Geologic and hydrologic hazards in glacierized basins in North America resulting from 19th and 20th century global warming, *Natural Hazards*, 8, 121/140, 1993.

565 Pearce, T. D., Ford, J. D., Laidler, G. J., Smit, B., Duerden, F., Allarut, M., Andrachuk, M., Baryluk, S., Dialla, A., Elee, P., Goose, A., Ikummaq, T., Joamie, E., Kataoyak, F., Loring, E., Meakin, S., Nickels, S., Shappa, K., Shirley, J., and Wandel, J.: Community collaboration and climate change research in the Canadian Arctic, *Polar Research*, 28, 10–27, <https://doi.org/10.1111/j.1751-8369.2008.00094.x>, 2009.

Richard L. Holmes: Computer-Assisted Quality Control in Tree-Ring Dating and Measurement, *Tree-Ring Bulletin*, 43, 1983.

570 Richardson, S. D. and Reynolds, J. M.: An overview of glacial hazards in the Himalayas, *Quaternary International*, 65–66, 31–47, [https://doi.org/10.1016/S1040-6182\(99\)00035-X](https://doi.org/10.1016/S1040-6182(99)00035-X), 2000.

Rinzin, S., Dunning, S., Carr, R. J., Sattar, A., and Mergili, M.: Exploring implications of input parameter uncertainties in glacial lake outburst flood (GLOF) modelling results using the modelling code r.avaflow, *Nat. Hazards Earth Syst. Sci.*, 25, 1841–1864, <https://doi.org/10.5194/nhess-25-1841-2025>, 2025.



575 Rounce, D. R., Hock, R., Maussion, F., Hugonnet, R., Kochtitzky, W., Huss, M., Berthier, E., Brinkerhoff, D., Compagno, L., Copland, L., Farinotti, D., Menounos, B., and McNabb, R. W.: Global glacier change in the 21st century: Every increase in temperature matters, *Science*, 379, 78–83, <https://doi.org/10.1126/science.abe1324>, 2023.

580 Sattar, A., Haritashya, U. K., Kargel, J. S., Leonard, G. J., Shugar, D. H., and Chase, D. V.: Modeling Lake Outburst and Downstream Hazard Assessment of the Lower Barun Glacial Lake, Nepal Himalaya, *Journal of Hydrology*, <https://doi.org/10.1016/j.jhydrol.2021.126208>, 2021.

Schuster, L., Maussion, F., Rounce, D. R., Ultee, L., Schmitt, P., Lacroix, F., Frölicher, T. L., and Schleussner, C.-F.: Irreversible glacier change and trough water for centuries after overshooting 1.5 °C, *Nat. Clim. Chang.*, <https://doi.org/10.1038/s41558-025-02318-w>, 2025.

585 Somos-Valenzuela, M. A., Chisolm, R. E., Rivas, D. S., Portocarrero, C., and McKinney, D. C.: Modeling a glacial lake outburst flood process chain: The case of Lake Palcacocha and Huaraz, Peru, *Hydrology and Earth System Sciences*, 20, 2519–2543, <https://doi.org/10.5194/hess-20-2519-2016>, 2016.

Stoffel, M. and Corona, C.: Dendroecological Dating of Geomorphic Disturbance in Trees, *Tree-Ring Research*, 70, 3–20, <https://doi.org/10.3959/1536-1098-70.1.3>, 2014.

Torrejón, F. and Bertrand, S.: Supplementan Information - Interviews regarding Baker GLOFs, 2021.

590 Troch, M., Åkesson, H., Cuzzzone, J. K., and Bertrand, S.: Precipitation drives western Patagonian glacier variability and may curb future ice mass loss, *Sci Rep*, 14, 26744, <https://doi.org/10.1038/s41598-024-77486-4>, 2024.

Turzewski, M. D., Huntington, K. W., and LeVeque, R. J.: The Geomorphic Impact of Outburst Floods: Integrating Observations and Numerical Simulations of the 2000 Yigong Flood, Eastern Himalaya, *JGR Earth Surface*, 124, 1056–1079, <https://doi.org/10.1029/2018JF004778>, 2019.

595 Vandekerkhove, E.: Impact of climate change on the occurrence of late Holocene glacial lake outburst floods in Patagonia: A sediment perspective, PhD thesis, Ghent University, Ghent, Belgium, 2021.

Vandekerkhove, E., Bertrand, S., Mauquoy, D., McWethy, D., Reid, B., Stammen, S., Saunders, K. M., and Torrejón, F.: Neoglacial increase in high-magnitude glacial lake outburst flood frequency, upper Baker River, Chilean Patagonia (47°S), *Quaternary Science Reviews*, 248, <https://doi.org/10.1016/j.quascirev.2020.106572>, 2020.

600 Wahl, T. L.: Uncertainty of Predictions of Embankment Dam Breach Parameters, *J. Hydraul. Eng.*, 130, 389–397, [https://doi.org/10.1061/\(ASCE\)0733-9429\(2004\)130:5\(389\)](https://doi.org/10.1061/(ASCE)0733-9429(2004)130:5(389)), 2004.

Wang, X., Zhang, G., Veh, G., Sattar, A., Wang, W., Allen, S. K., Bolch, T., Peng, M., and Xu, F.: Reconstructing glacial lake outburst floods in the Poiqu River basin, central Himalaya, *Geomorphology*, 449, 109063, <https://doi.org/10.1016/j.geomorph.2024.109063>, 2024.

605 Westoby, M. J., Glasser, N. F., Brasington, J., Hambrey, M. J., Quincey, D. J., and Reynolds, J. M.: Modelling outburst floods from moraine-dammed glacial lakes, *Earth-Science Reviews*, 134, 137–159, <https://doi.org/10.1016/j.earscirev.2014.03.009>, 2014.

Williams, R. D., Griffiths, H. M., Carr, J. R., Hepburn, A. J., Gibson, M., Williams, J. J., and Irvine-Fynn, T. D. L.: Integrating historical, geomorphological and sedimentological insights to reconstruct past floods: Insights from Kea Point, Mt. Cook Village, Aotearoa New Zealand, *Geomorphology*, 398, <https://doi.org/10.1016/j.geomorph.2021.108028>, 2022.